Electronic Supplementary Material (ESI) for Physical Chemistry Chemical Physics.

Calculation of the Permeability Coefficients of Small Molecules Through Lipid Bilayers by Free-Energy Reaction Network Analysis Following the Explicit Treatment of the Internal Conformation of the Solute

Yuki Mitsuta, Toshio Asada* and Yasuteru Shigeta†*

*Graduate School of Science, Osaka Prefecture University, 1–1, Gakuenmach, Nakaku, Osaka, Japan, 599–8531

Email: mitsutay@c.s.osakafu–u.ac.jp

Frequency Factor of Rate Constant

In the calculation of rate constants, we defined two type frequency factors: A_θ in equation (8) and A_z in equation (9). Theoretical estimation is challenging because it is dependent on the viscosity of the liquid solvent. As a result, we use the enhanced sampling method to evaluate these factors. In a previous study, we demonstrated how to calculate the frequency factor using the enhanced sampling trajectory[1], which is based on the method of METAGUI tool[2,3]. This method was modified in this case. When the target distribution is defined as sufficiently flattened in our VES sampling, the goal of the enhanced sampling is to make the distribution flatten, i.e., to obtain the flatten potential. At the end of the simulation, it is possible to determine whether the trajectory is considered to be motion on flatten potential, i.e., Brownian motion. In Einstein–Smoluchowski equation, the diffusion constant of the sampling is calculated as,

$$D_x = \lim_{t\to\infty} \frac{\langle |x(t) - x(0)|^2 \rangle}{2nt} . \quad \text{(S1)}$$

where n denotes the dimension For the internal degrees of freedom, $x(t) = \{\phi,\psi,\chi_1,\chi_2\}$ and $n = 4$, while for the permutation direction, $x(t) = z(t)$ and $n = 1$ in the present case. In practice, the limitation of $t\to\infty$ cannot be applied directly because of the periodicity of the CVs. D_x is calculated by the slope of the line in plot of time vs $\langle |x(t) - x(0)|^2 \rangle$. This term is calculated by the next three steps. (1) the trajectory of sampling trajectory is separated for each stride Δt. (2) $|x(t) - x(0)|^2$ is calculated for each time with the time step δt. (3) The average of step (2) is calculated and plotted every time. In addition, the frequency factors of the inner and outer sides of the membrane should be different because of the difference in viscosity. Here, we defined the inner region as $|z| < 25$ and the outer one as $|z| \geq 25$. Δt and δt were chosen to estimate by the linear dependency. For the solute conformation (D_θ), we choose $\Delta t = 10$ fs and $\delta t = 2$ fs, and the additional simulation was performed from the end of the VES calculation in 1 ns × 36 walkers to estimate them. For the time range of the permeation (D_z), we chose $\delta t = 1$ ns and $\Delta t = 100$ ns for the inner side of the membrane and $\Delta t = 10$ ns for outer side, and the trajectory is last 50 ns × 36 walkers simulation of the VES calculation. The plots of time vs $\langle |x(t) - x(0)|^2 \rangle$ are shown in Figure S1, and these selections show the linear dependency. Then, the frequency factors can be calculated as,

$$A_x = \frac{D_x}{d_x}, \quad \text{(S2)}$$

with d_x denotes the distance between two states, which is explained main text.

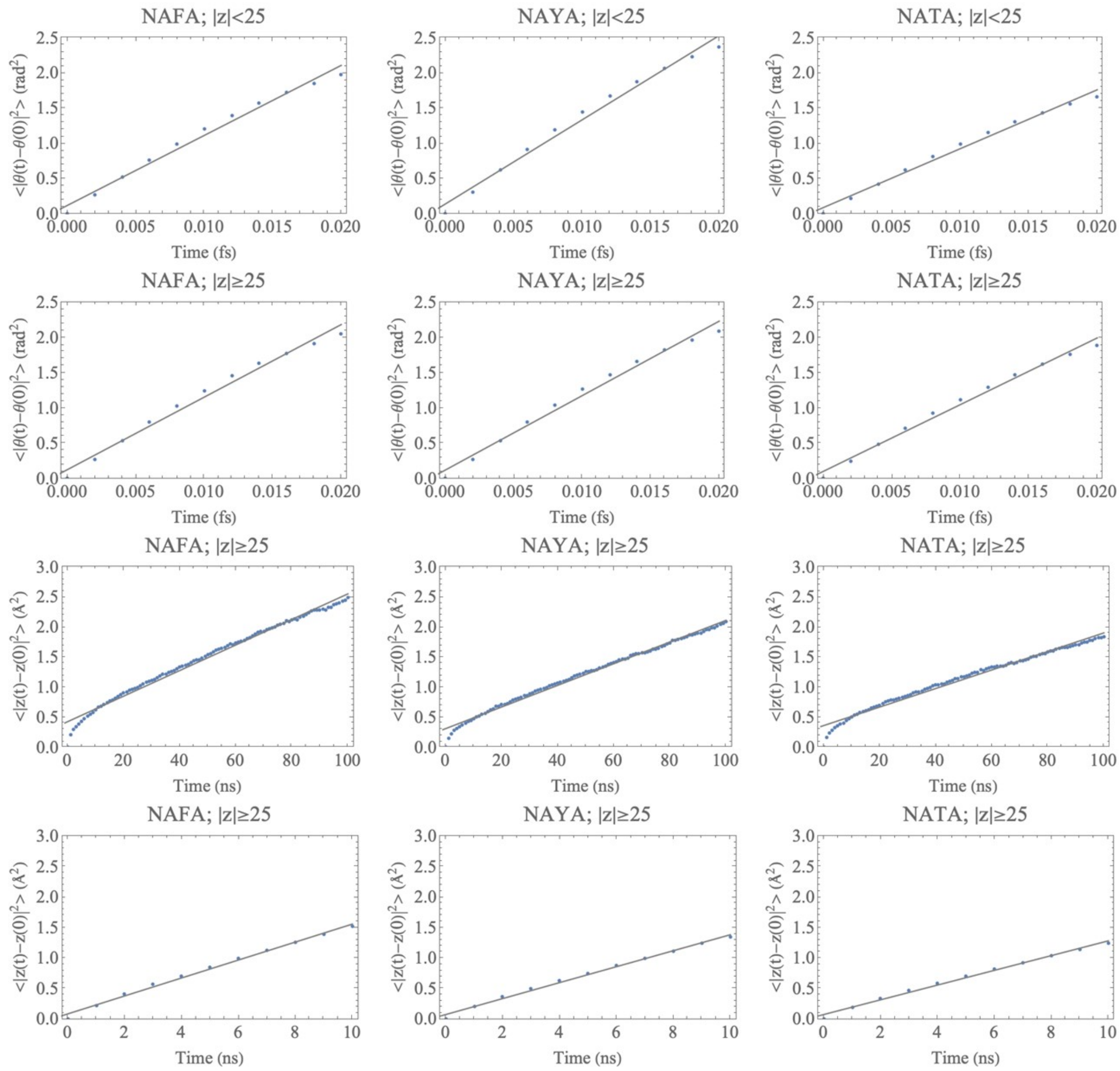

Figure S1. The plot of time vs $\langle|x(t) - x(0)|^2\rangle$, with x is the inner conformation ($\theta(t)$) or the permutation direction ($z(t)$). The blue points are the result of sampling, and the gray lines are linear regression.

Table S1. Frequency factor of each molecule for the inner conformation A_θ and the permutation direction A_z. The result is separated in the inner of the membrane as $|z| < 25$ Å, and the outer as $|z| \geq 25$ Å. The range of frequency factors were evaluated by using the standard deviations of $\langle |x(t) - x(0)|^2 \rangle$.

	Inner ($|z| < 25$ Å)			
	A_θ (rad/ps)		A_z (Å/ps)	
	Average	Range	Average	Range
NAFA	12.89	12.85 – 12.93	9.62×10^{-3}	9.46×10^{-3} – 9.77
NAYA	13.38	13.38 – 13.41	7.50×10^{-3}	7.37×10^{-3} – 7.63
NATA	13.13	13.09 – 13.17	7.85×10^{-3}	7.68×10^{-3} – 8.02

	Outer ($|z| \geq 25$ Å)			
	A_θ (rad/ps)		A_z (Å/ps)	
	Average	Range	Average	Range
NAFA	11.53	11.45 – 11.61	7.75×10^{-2}	7.67×10^{-2} – 7.83
NAYA	13.16	13.05 – 13.26	6.75×10^{-2}	6.69×10^{-3} – 6.81
NATA	12.36	12.29 – 12.43	6.54×10^{-2}	6.50×10^{-3} – 6.59

Convergence of Variationally Enhances Sampling Calculation

The variationally enhanced sampling (VES) method is a relatively new method, and we should consider simulation convergence. In our study, we chose a flatten distribution as the target distribution, and the convergence can be estimated using the distribution of MD simulation converged to the flatten distribution. Figures S2 and S3 depict the contour plot of the sampling between two CVs during the final 100 ns × 36 walker simulation. All areas have been sampled.

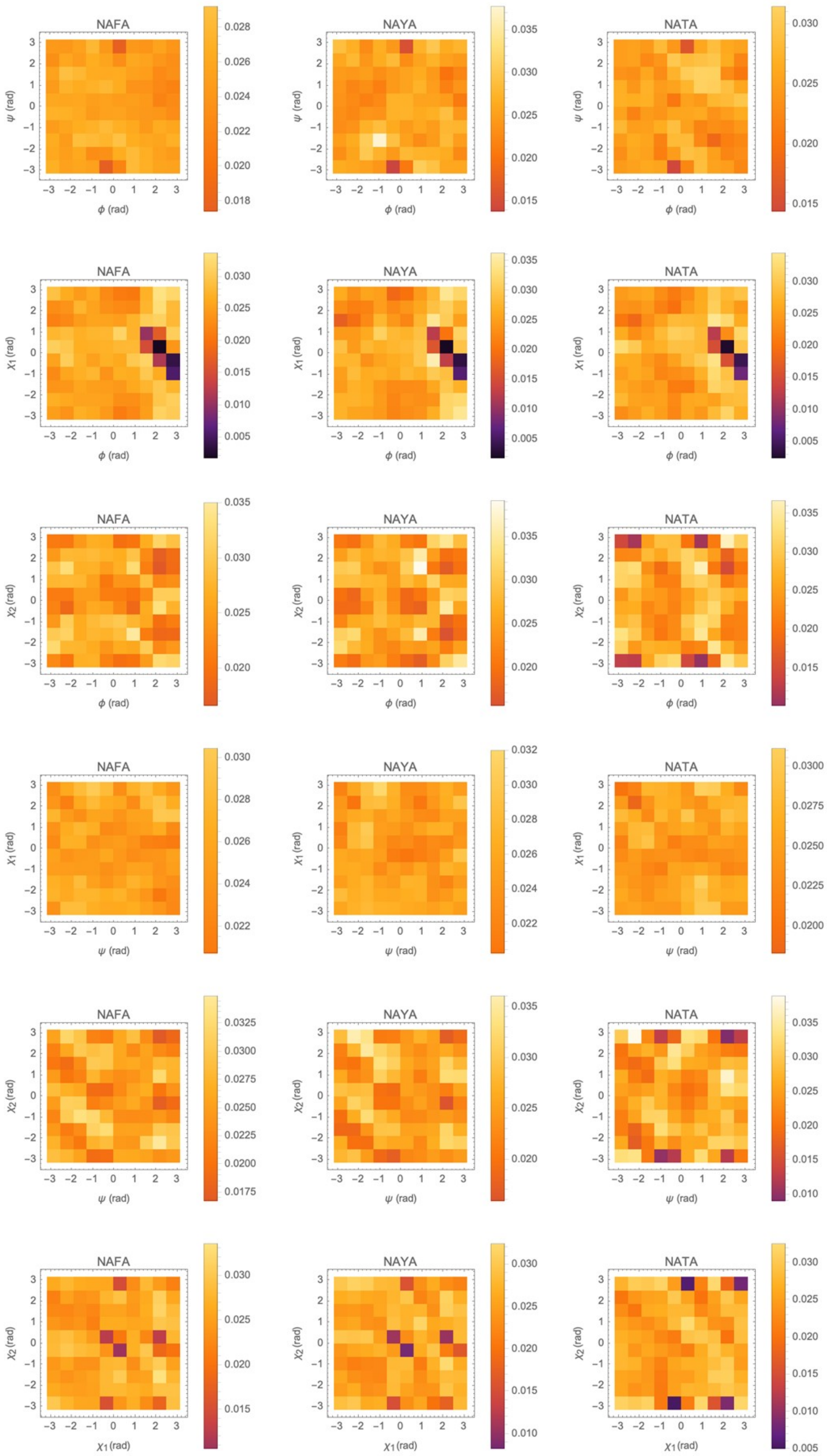

Figure S2. Contour plot of the probability density functions for the samplings in two inner angles.

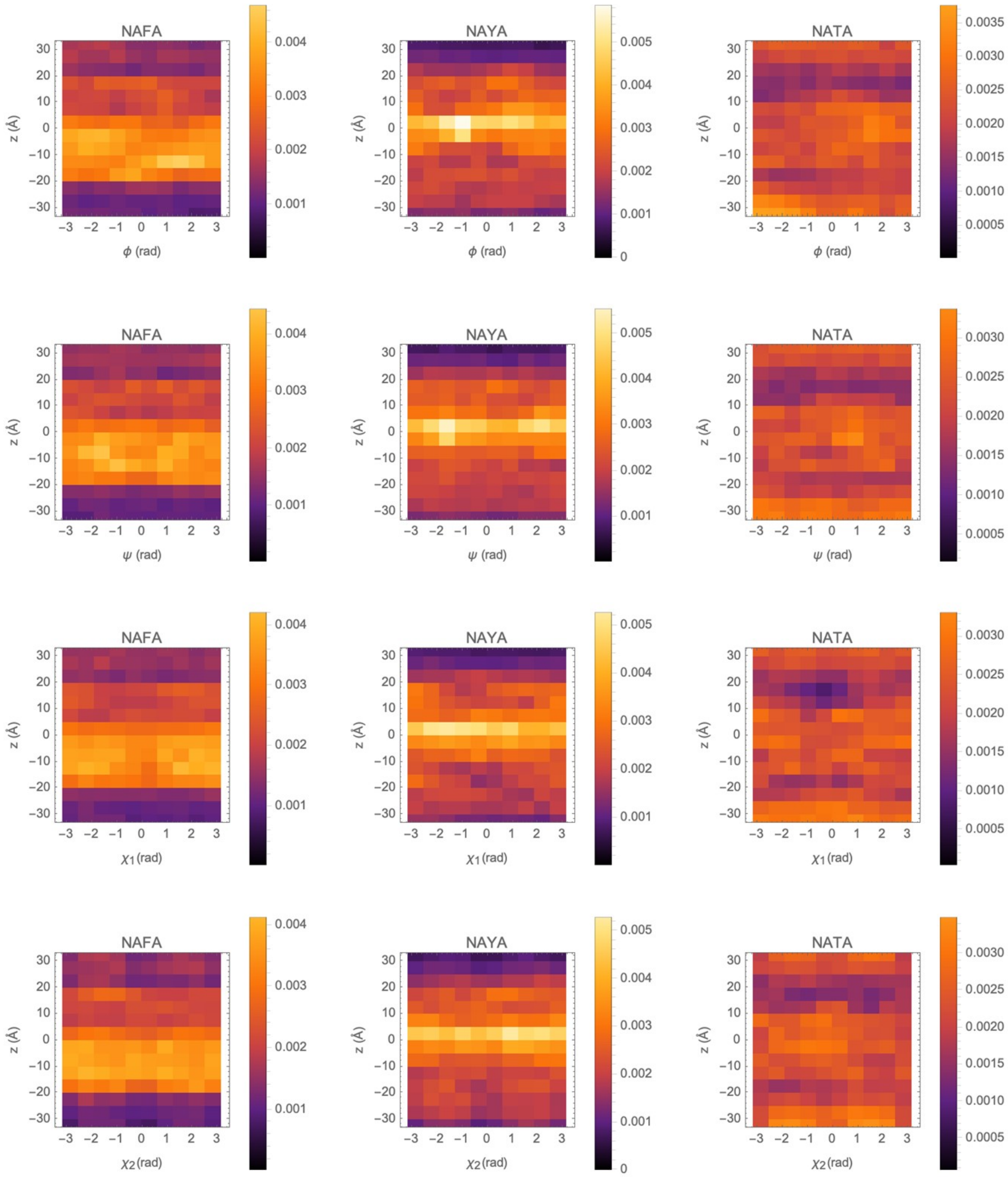

Figure S3. Contour plot of the probability density functions for the samplings in each inner angles and direction of the permutation (z).

Bias Potential of VES Calculation

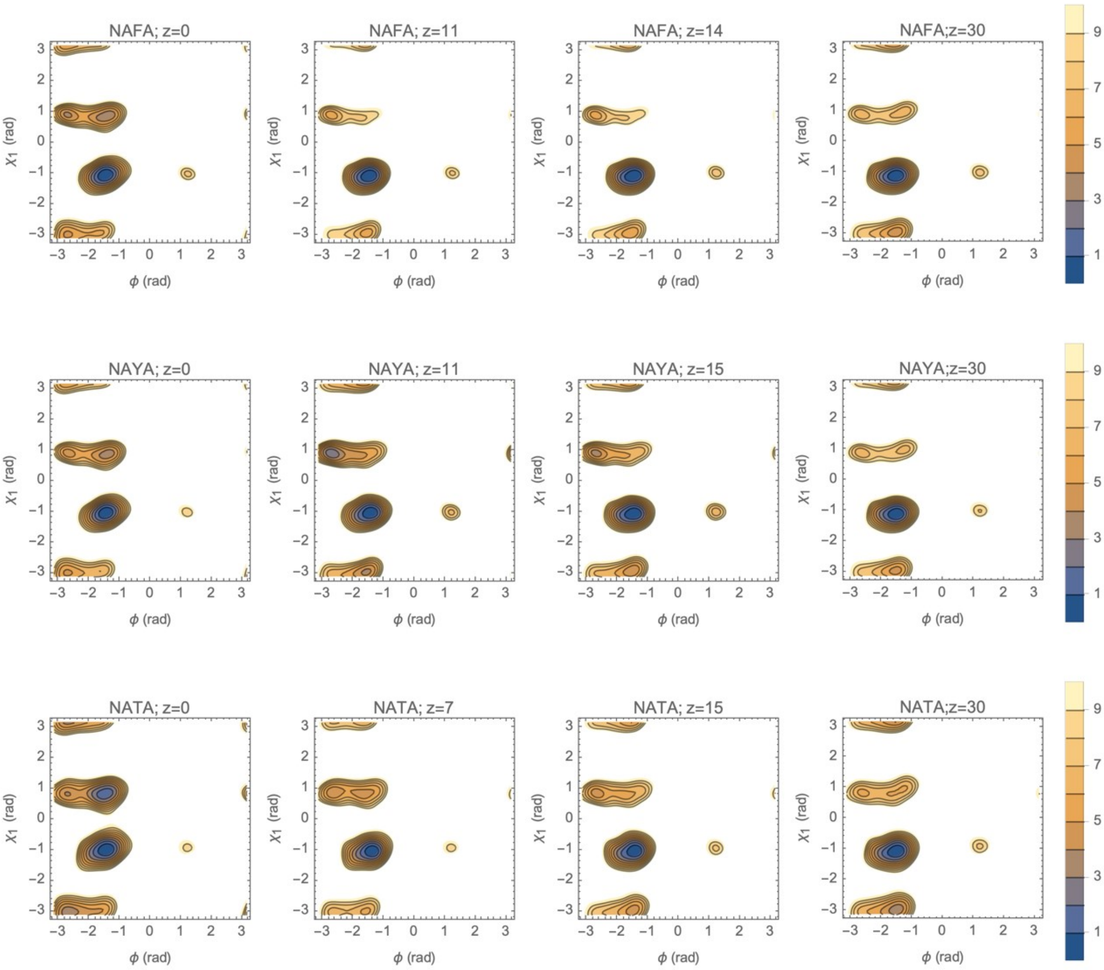

Figure S4. Contour plots of potential for Ramachandran plots, which is $V_2(\phi,\chi_1,z)$ in equation (14). The unit of potential is kJ/mol. The displacement from the center of the bilayer (z) are selected the area of water ($z = 30$ Å) the interface of the lipid bilayer ($z = 14$ Å for NAFA and NAYA, $z = 15$ Å for NATA), the crossing area of the stable inner structure that is shown Figure 5 ($z = 10$ Å for NAFA and NAYA, $z = 8$ Å for NATA) and the center of the bilayer ($z = 0$ Å).

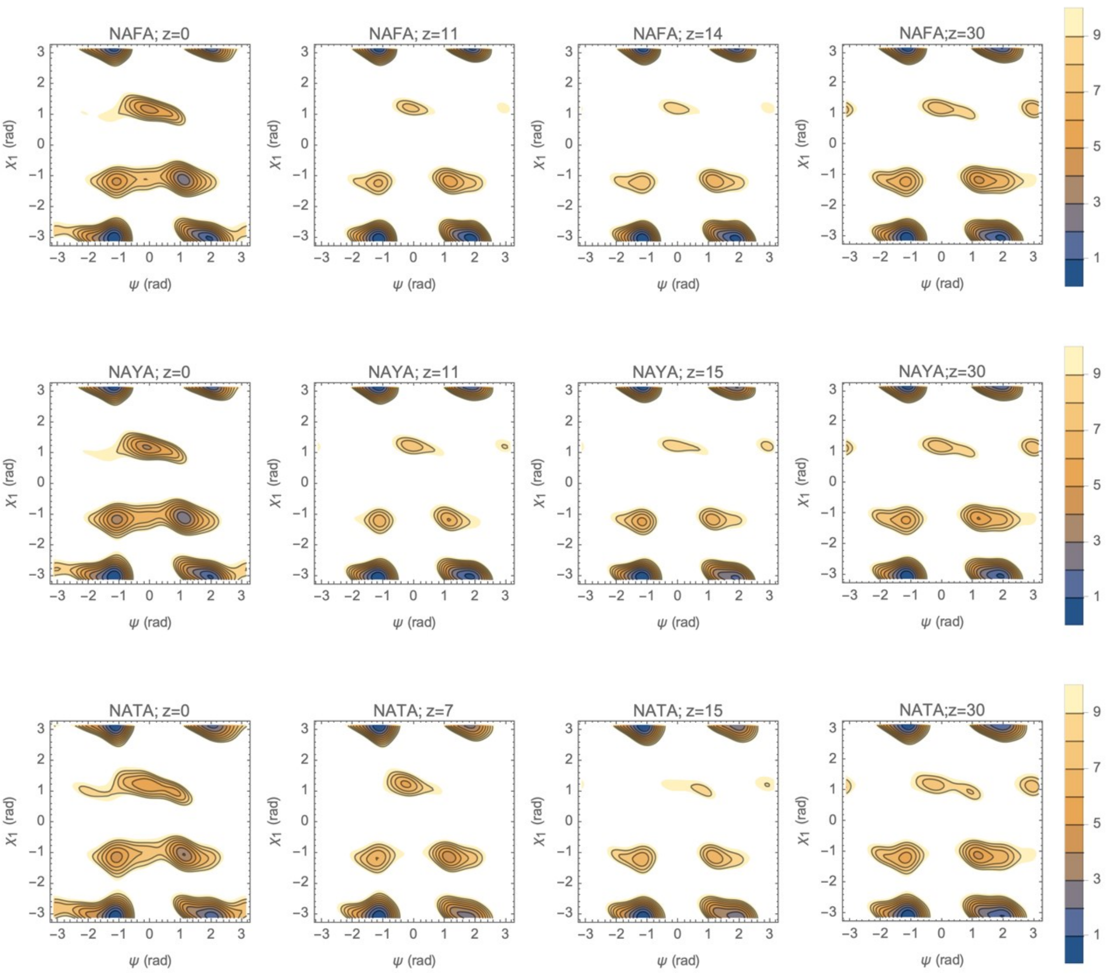

Figure S5. Contour plots of potential for Ramachandran plots, which is $V_3(\psi,\chi_1,z)$ in equation (15). The unit of potential is kJ/mol. The displacement from the center of the bilayer (z) are selected the area of water (z = 30 Å), the interface of the lipid bilayer (z = 14 Å for NAFA and NAYA, z = 15 Å for NATA), the crossing area of the stable inner structure that is shown Figure 5 (z = 10 Å for NAFA and NAYA, z = 8 Å for NATA) and the center of the bilayer (z = 0 Å).

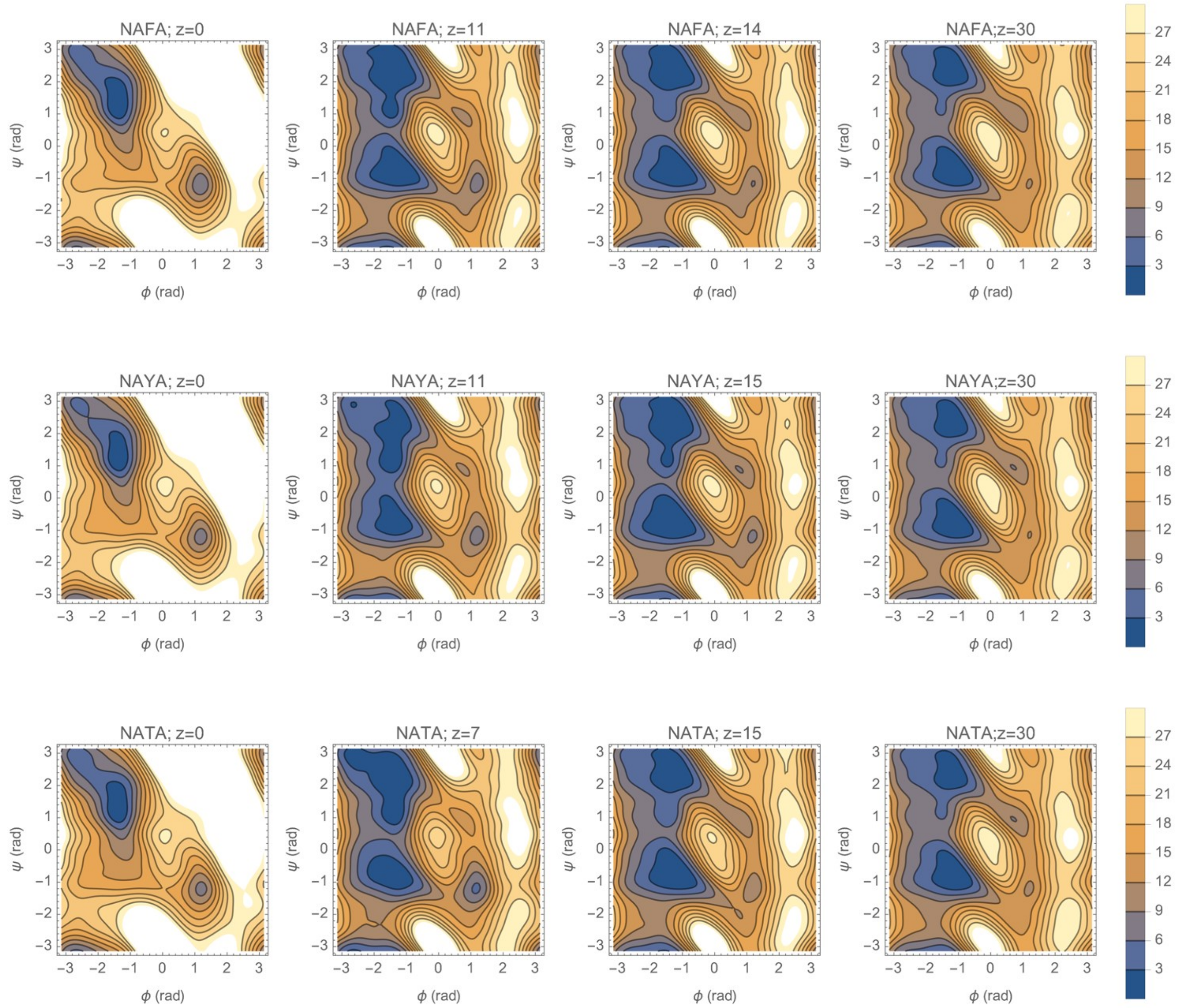

Figure S6. Contour plots of the potential of the Ramachandran plots, which is represented by $V_1(\phi,\psi,z)$ in Equation (15). The potential is same with Figure 6 and the range of contour plot is changed from 0–10 kJ/mol to 0–30 kJ/mol.

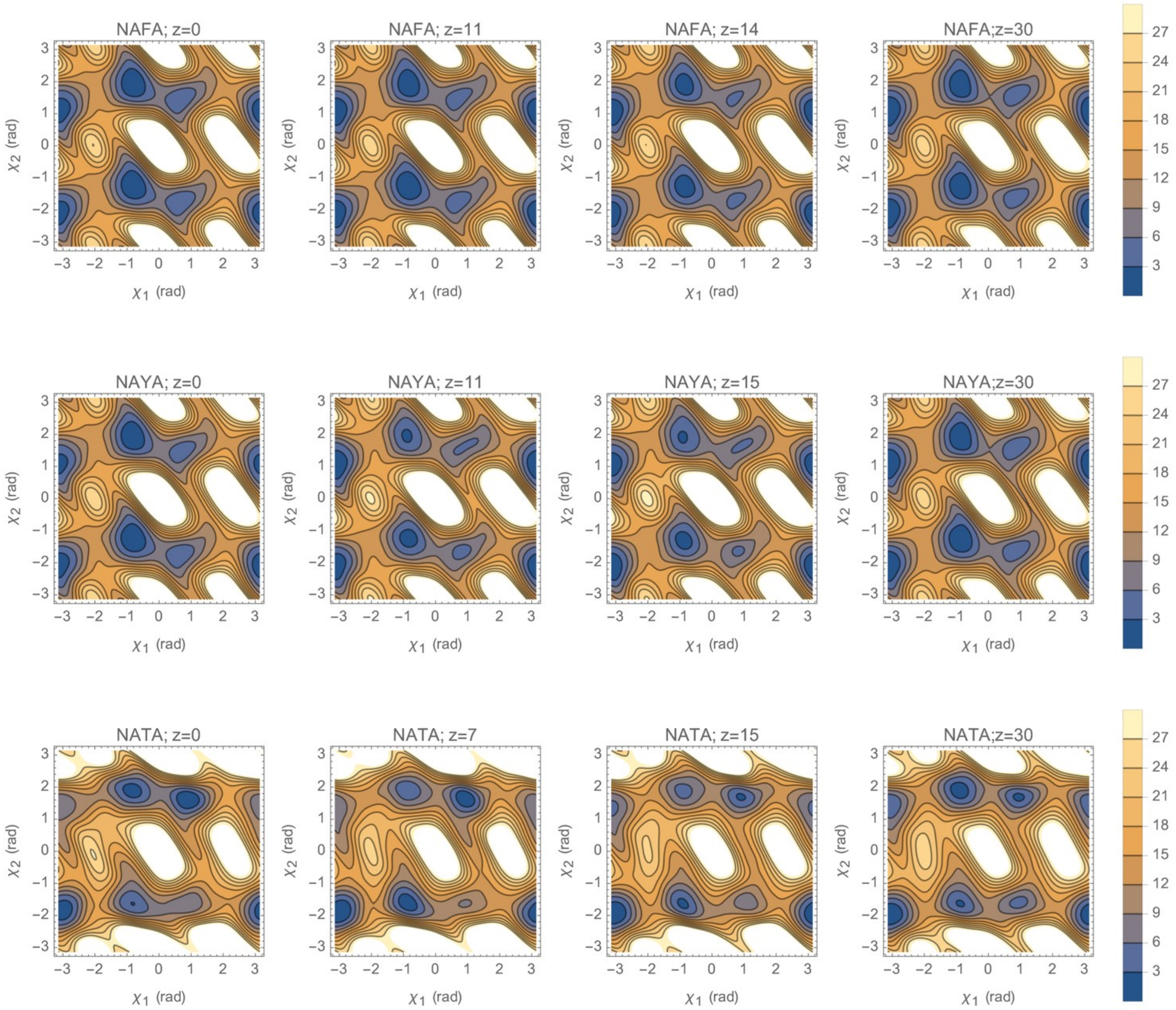

Figure S7. Contour plots of the potential of the peptide side-chain conformations, which is $V_4(\chi_1,\chi_2,z)$ in Equation (15). The potential is same with Figure 7 and the range of contour plot is changed from 0–10 kJ/mol to 0–30 kJ/mol.

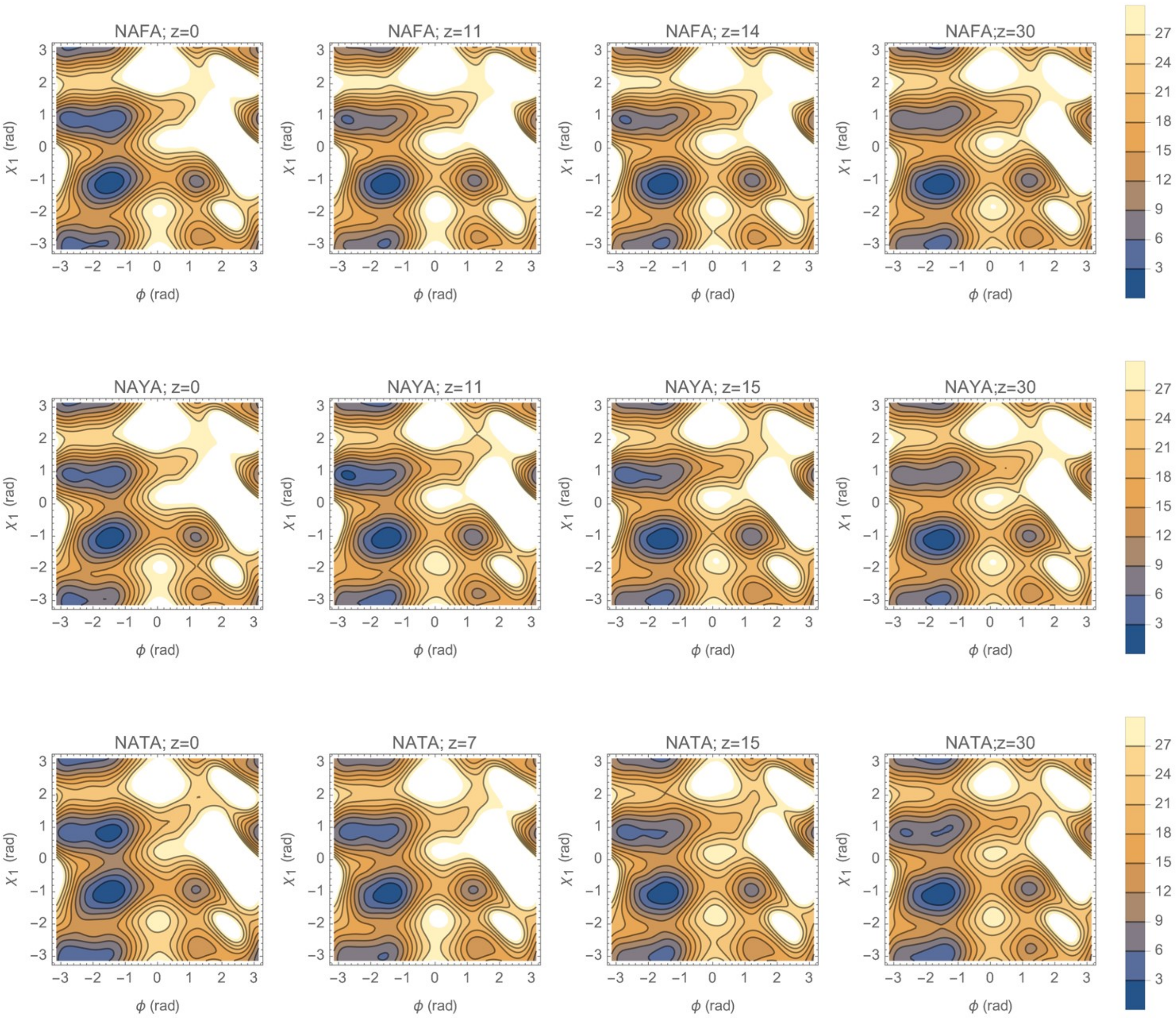

Figure S8. Contour plots of potential for Ramachandran plots, which is $V_2(\phi,\chi_1,z)$ The potential is same with Figure S4 and the range of contour plot is changed from 0–10 kJ/mol to 0–30 kJ/mol.

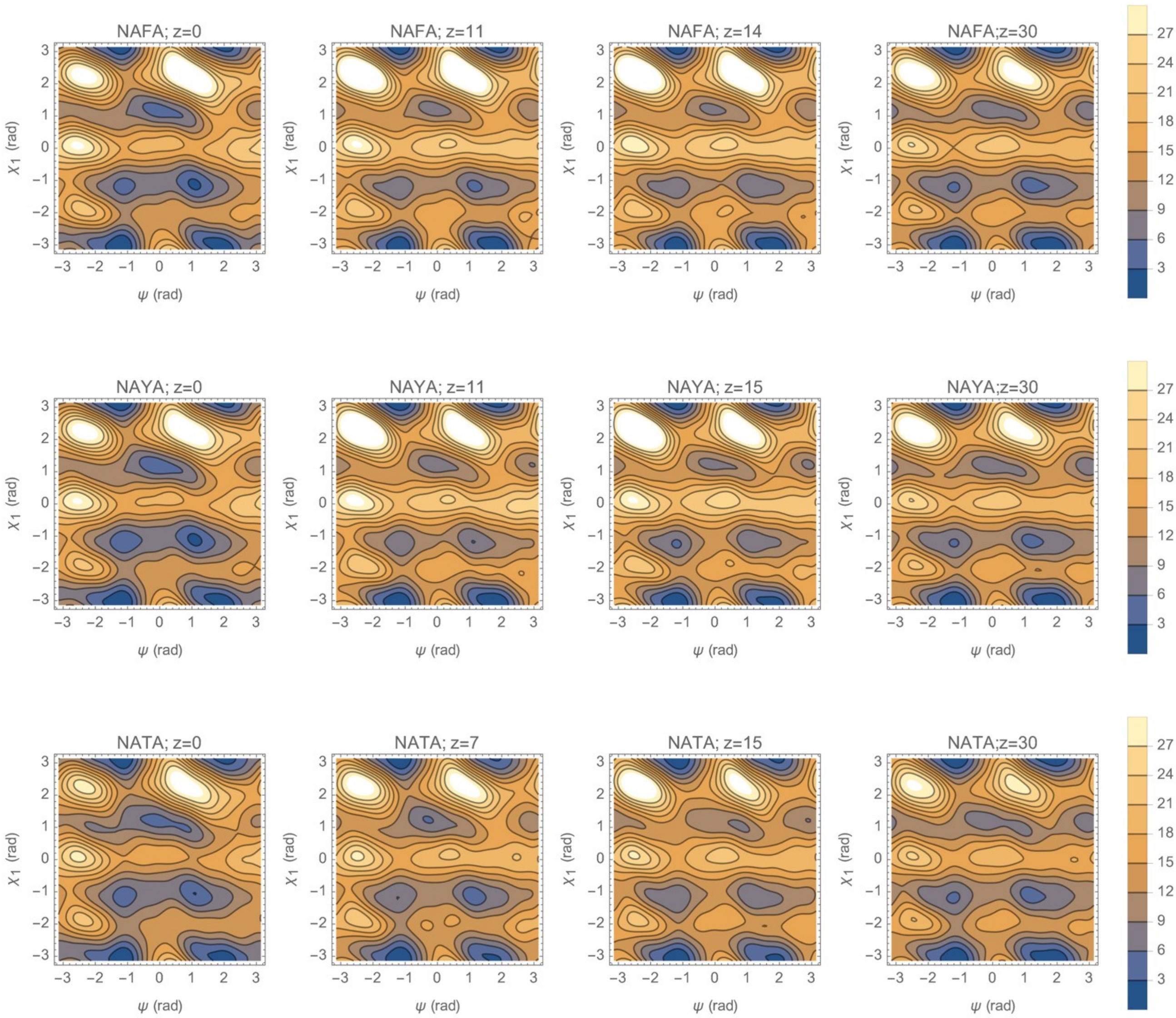

Figure S9. Contour plots of potential for Ramachandran plots, which is $V_3(\psi,\chi_1,z)$ The potential is same with Figure S5 and the range of contour plot is changed from 0–10 kJ/mol to 0–30 kJ/mol.

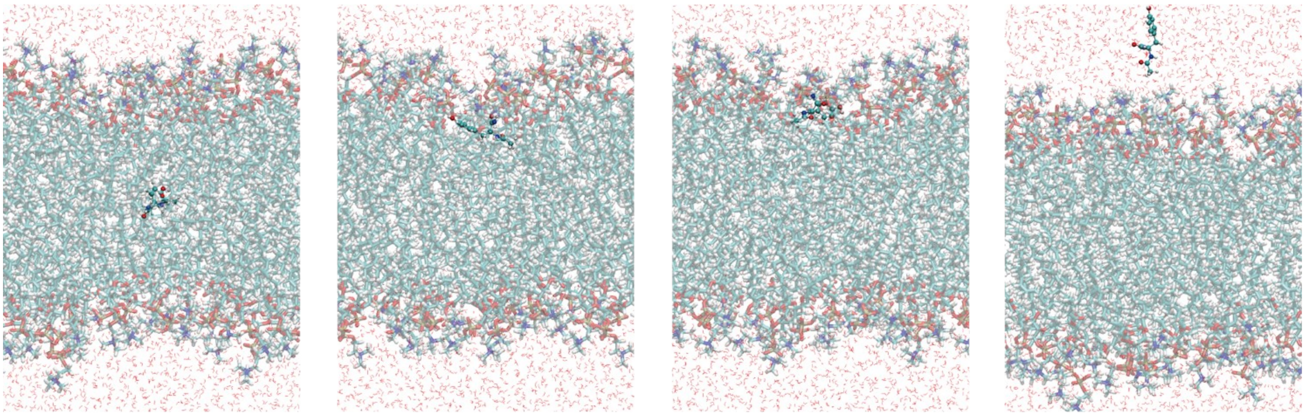

Z = 0 Å　　Z = 11 Å　　Z = 15 Å　　Z = 30 Å

Figure S10. Snapshot of the permeation of the NAYA through DOPC bilayer system.

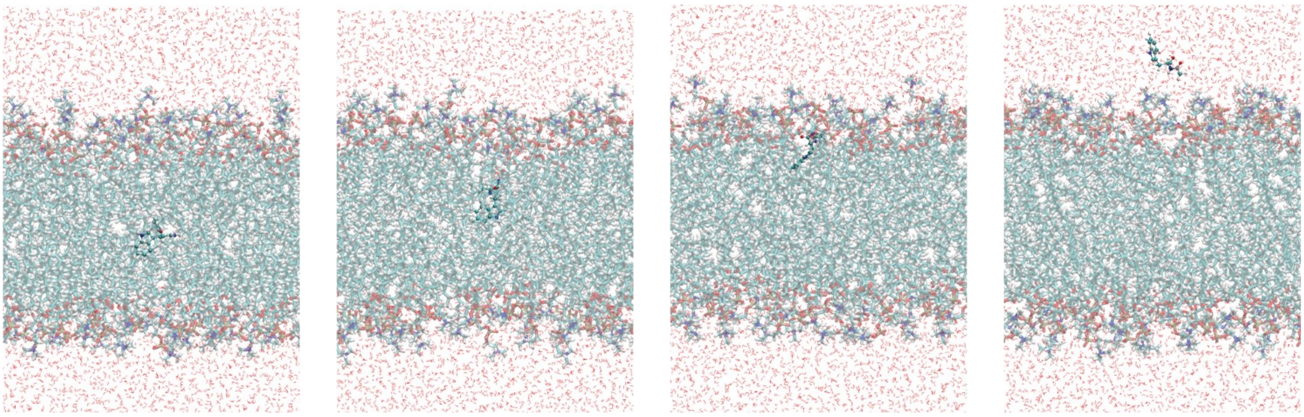

Z = 0 Å　　Z = 7 Å　　Z = 15 Å　　Z = 30 Å

Figure S11. Snapshot of the permeation of the NATA through DOPC bilayer system.

Table S2. CVs of inner structures and bias potentials of the EQ points of the NAFA in $z = 0$ Å.

ϕ (rad)	ψ (rad)	χ_1 (rad)	χ_2 (rad)	$V(s)$ (kJ/mol)
–1.410	1.149	–1.010	–1.210	–48.0
–1.410	1.150	–1.013	1.950	–47.8
–1.554	1.860	–3.011	1.116	–42.3
–1.556	1.864	–3.016	–2.083	–41.8
–1.385	1.026	0.838	–1.681	–36.0
–1.386	1.027	0.837	1.518	–35.8
1.199	–1.153	–1.007	–1.210	–31.3
1.199	–1.153	–1.009	1.950	–31.1
1.229	–1.185	–2.947	1.134	–29.2
1.229	–1.185	–2.948	–2.045	–28.7
–1.391	–0.910	–1.010	–1.210	–28.5
–1.391	–0.910	–1.013	1.950	–28.3
–2.677	2.974	0.939	–1.649	–28.0
–2.678	2.974	0.946	1.573	–27.9
–1.611	–1.063	–3.017	1.114	–26.7
–2.562	–1.148	–3.040	1.109	–26.6
–1.613	–1.063	–3.023	–2.087	–26.2
–2.562	–1.148	–3.048	–2.098	–26.2
–2.678	2.974	0.944	0.324	–19.9
–2.675	2.973	0.929	–2.810	–19.9
–2.608	–1.148	0.869	–1.672	–15.2
–2.608	–1.148	0.870	1.535	–15.1
1.073	0.865	–0.973	–1.212	–10.3
1.073	0.865	–0.975	1.951	–10.1
0.960	–1.112	1.138	1.657	–2.2
0.935	–1.144	1.098	–1.591	–2.0
1.155	1.152	–2.857	1.167	1.0
1.156	1.150	–2.854	–1.996	1.5
1.281	1.800	–2.944	1.136	1.8
1.281	1.800	–2.944	–2.043	2.3

Table S3. CVs of inner structures and bias potentials of the EQ points of the NAFA in $z = 30$ Å.

ϕ (rad)	ψ (rad)	χ_1 (rad)	χ_2 (rad)	$V(s)$ (kJ/mol)
–1.422	–1.039	–3.030	1.099	–63.3
–1.422	–1.038	–3.031	–2.100	–63.1
–1.462	2.041	–3.034	1.099	–62.5
–1.462	2.042	–3.035	–2.101	–62.3
–1.404	–1.008	–1.057	–1.243	–61.0
–1.404	–1.008	–1.059	1.893	–60.9
–1.437	2.078	–1.059	–1.243	–60.2
–1.437	2.078	–1.061	1.894	–60.2
–1.523	1.154	–1.055	–1.244	–58.7
–1.523	1.154	–1.057	1.893	–58.7
–1.446	2.757	–1.056	1.893	–57.7
–1.289	2.881	1.029	1.658	–50.2
–1.260	–0.314	1.057	1.669	–50.1
–1.293	2.883	1.016	–1.566	–50.0
–1.265	–0.309	1.043	–1.556	–49.9
–2.592	2.960	0.976	1.637	–46.7
–2.590	2.961	0.965	–1.583	–46.7
–1.485	0.997	0.911	–1.598	–45.3
–1.481	0.993	0.921	1.617	–45.3
1.011	0.972	–0.999	–1.255	–44.5
1.011	0.972	–1.001	1.881	–44.5
1.212	–1.164	–2.977	1.105	–44.3
1.212	–1.164	–2.976	–2.084	–44.1
1.200	–1.178	–1.016	–1.251	–44.0
1.200	–1.178	–1.018	1.885	–44.0
–2.476	0.954	0.899	–1.601	–42.9
–2.478	0.950	0.908	1.612	–42.9
–1.250	–0.326	1.090	0.046	–42.7
–1.249	–0.327	1.093	–3.114	–42.7
–1.281	2.876	1.057	0.097	–42.7
–1.280	2.876	1.060	–3.069	–42.6

Table S3. CVs of inner structures and bias potentials of the EQ points of the NAFA in $z = 30$ Å. Continued.

ϕ (rad)	ψ (rad)	χ_1 (rad)	χ_2 (rad)	$V(s)$ (kJ/mol)
1.069	–1.939	–1.016	–1.251	–40.6
1.025	1.145	–2.936	1.111	–39.6
1.025	1.144	–2.934	–2.072	–39.3
–2.593	2.960	0.989	0.203	–39.1
–2.594	2.960	0.991	–2.974	–39.0
–1.485	0.996	0.913	0.331	–37.6
–1.482	0.994	0.918	–2.861	–37.5
1.195	2.977	–1.007	–1.253	–36.1
1.195	2.976	–1.009	1.883	–36.1
–2.433	–2.050	0.898	–1.601	–35.4
–2.438	–2.074	0.908	1.612	–35.4
–2.475	0.958	0.892	0.371	–35.2
–2.476	0.955	0.897	–2.822	–35.1
0.627	0.931	1.007	1.649	–29.9
0.625	0.935	0.995	–1.573	–29.8
–2.427	–2.029	0.890	–2.809	–27.7
0.615	–2.065	1.000	1.647	–24.0
0.613	–2.054	0.988	–1.576	–23.9
0.631	0.924	1.028	0.141	–22.3
0.631	0.923	1.030	–3.029	–22.3
0.954	3.116	1.153	1.706	–20.3
0.948	3.121	1.141	–1.513	–20.0
0.620	–2.083	1.020	0.154	–16.4
0.620	–2.086	1.023	–3.018	–16.4
0.985	3.094	1.217	2.988	–13.4
0.983	3.095	1.214	–0.153	–13.4

Table S4. CVs of inner structures and bias potentials of the EQ points of the NAYA in $z = 0$ Å.

ϕ (rad)	ψ (rad)	χ_1 (rad)	χ_2 (rad)	$V(s)$ (kJ/mol)
–1.401	1.148	–1.003	–1.222	–36.0
–1.402	1.149	–1.008	1.944	–35.9
–1.526	1.888	–3.012	–2.047	–28.4
–1.525	1.887	–3.009	1.105	–28.1
–1.378	1.049	0.835	–1.685	–23.4
–1.377	1.044	0.847	1.524	–23.1
1.191	–1.154	–1.009	–1.222	–18.7
1.192	–1.154	–1.014	1.945	–18.6
–1.402	–0.922	–1.008	–1.222	–18.2
–1.403	–0.923	–1.014	1.945	–18.1
1.231	–1.187	–2.949	–2.014	–15.0
1.231	–1.187	–2.951	1.123	–14.7
–1.579	–1.039	–3.021	–2.053	–14.3
–2.447	–1.090	–3.051	–2.068	–14.2
–2.667	2.964	0.939	–1.656	–14.1
–2.670	2.964	0.957	1.577	–14.1
–1.578	–1.039	–3.018	1.103	–14.0
–2.447	–1.090	–3.046	1.096	–13.8
–2.669	2.964	0.953	–2.869	–6.6
–2.668	2.964	0.946	0.330	–6.1
–2.493	–0.997	0.883	–1.672	–2.5
1.038	0.894	–0.972	–1.224	2.3
1.039	0.897	–0.978	1.940	2.4
0.980	–1.115	1.161	1.671	10.4
0.936	–1.181	1.091	–1.602	10.8
1.139	1.220	–2.863	–1.977	13.5
1.238	1.770	–2.937	–2.008	13.7
1.139	1.225	–2.870	1.150	13.9
1.239	1.774	–2.940	1.127	14.0
1.034	–0.955	1.298	2.875	16.8

Table S5. CVs of inner structures and bias potentials of the EQ points of the NAYA in $z = 30$ Å.

ϕ (rad)	ψ (rad)	χ_1 (rad)	χ_2 (rad)	$V(s)$ (kJ/mol)
–1.416	–1.039	–3.031	1.095	–66.0
–1.417	–1.038	–3.034	–2.097	–65.8
–1.455	2.037	–3.031	1.095	–64.8
–1.456	2.038	–3.034	–2.097	–64.6
–1.398	–1.007	–1.056	–1.245	–63.9
–1.398	–1.007	–1.055	1.901	–63.7
–1.431	2.073	–1.056	–1.244	–62.8
–1.431	2.073	–1.056	1.901	–62.6
–1.519	1.148	–1.049	–1.245	–61.5
–1.519	1.148	–1.049	1.900	–61.3
–1.445	2.817	–1.051	1.900	–60.1
–1.260	–0.318	1.068	1.680	–52.6
–1.280	2.883	1.039	1.668	–52.5
–1.261	–0.317	1.063	–1.547	–52.5
–1.281	2.884	1.035	–1.558	–52.4
–2.604	2.962	0.973	1.639	–49.5
–2.604	2.962	0.971	–1.580	–49.4
–1.479	1.001	0.928	1.620	–47.8
–1.479	1.001	0.927	–1.592	–47.7
1.002	0.963	–0.991	–1.252	–47.3
1.002	0.963	–0.992	1.888	–47.1
1.218	–1.154	–2.980	1.098	–46.8
1.218	–1.154	–2.980	–2.081	–46.6
1.202	–1.171	–1.014	–1.249	–46.3
1.202	–1.171	–1.015	1.893	–46.1
–2.485	0.959	0.901	1.609	–45.5
–1.249	–0.332	1.105	–3.136	–45.5
–2.485	0.959	0.902	–1.599	–45.5
–1.271	2.878	1.071	–3.091	–45.3
–1.248	–0.334	1.109	0.020	–45.2
–1.270	2.877	1.076	0.070	–45.0
1.065	–1.973	–1.007	–1.250	–42.9

Table S5. CVs of inner structures and bias potentials of the EQ points of the NAYA in $z = 30$ Å. Continued.

ϕ (rad)	ψ (rad)	χ_1 (rad)	χ_2 (rad)	$V(s)$ (kJ/mol)
1.065	–1.973	–1.008	1.891	–42.7
–2.607	2.961	0.991	–2.981	–42.0
1.017	1.142	–2.942	1.103	–42.0
1.017	1.141	–2.939	–2.069	–41.8
–2.607	2.961	0.998	0.189	–41.7
–1.475	0.997	0.937	–2.901	–40.3
–1.473	0.995	0.943	0.279	–39.8
1.201	2.958	–1.006	–1.250	–38.6
1.201	2.958	–1.006	1.891	–38.4
–2.484	0.960	0.899	–2.838	–38.0
–2.427	–2.060	0.900	1.609	–38.0
–2.427	–2.061	0.900	–1.599	–37.9
–2.484	0.960	0.899	0.362	–37.6
0.634	0.935	1.005	1.653	–33.0
0.633	0.936	1.002	–1.570	–32.9
–2.425	–2.050	0.894	–2.830	–30.4
0.619	–2.082	1.001	1.652	–26.5
0.619	–2.079	0.998	–1.571	–26.5
0.639	0.927	1.029	–3.034	–25.6
0.640	0.925	1.036	0.131	–25.3
0.960	3.098	1.156	1.716	–23.2
0.958	3.100	1.151	–1.508	–23.0
0.627	–2.108	1.028	–3.031	–19.2
0.629	–2.115	1.035	0.133	–18.8
0.987	3.077	1.213	2.990	–16.6
0.989	3.075	1.217	–0.153	–16.3

Table S6. CVs of inner structures and bias potentials of the EQ points of the NATA in $z = 0$ Å.

ϕ (rad)	ψ (rad)	χ_1 (rad)	χ_2 (rad)	$V(s)$ (kJ/mol)
–1.405	1.150	–0.977	1.918	–38.4
–1.405	1.150	–0.976	–1.607	–36.7
–1.404	1.077	0.865	1.621	–35.1
–1.536	1.887	–3.005	–1.841	–34.0
–1.463	1.414	–2.952	–1.830	–33.7
–1.405	1.080	0.857	–1.656	–29.0
–1.542	1.894	–3.025	1.456	–28.1
–1.466	1.439	–2.967	1.449	–27.8
–1.540	1.892	–3.018	0.367	–24.3
–1.465	1.434	–2.964	0.282	–24.0
–2.673	2.946	0.940	1.616	–22.7
–1.407	–0.882	–0.968	1.917	–21.6
–1.656	–1.018	–3.023	–1.844	–21.5
–2.387	–1.057	–3.037	–1.847	–21.4
1.222	–1.170	–2.948	–1.830	–20.5
1.201	–1.166	–0.950	1.914	–20.3
–1.407	–0.881	–0.967	–1.608	–19.9
–1.785	2.791	0.912	1.618	–19.7
1.201	–1.166	–0.949	–1.611	–18.6
–2.672	2.947	0.950	–1.640	–16.6
–1.670	–1.019	–3.045	1.458	–15.7
–2.385	–1.057	–3.058	1.460	–15.6
1.221	–1.171	–2.962	1.448	–14.6
–1.798	2.800	0.916	–1.646	–13.6
–1.666	–1.019	–3.039	0.406	–11.8
–2.385	–1.057	–3.056	0.447	–11.7
1.221	–1.171	–2.960	0.276	–10.8
1.005	0.890	–0.921	1.909	–1.5
1.005	0.889	–0.919	–1.616	0.2
1.012	–1.096	1.163	1.604	1.8
1.090	1.099	–2.839	–1.805	5.9
1.023	–1.059	1.231	–1.603	7.1

Table S6. CVs of inner structures and bias potentials of the EQ points of the NATA in $z = 0$ Å.

Continued.

ϕ (rad)	ψ (rad)	χ_1 (rad)	χ_2 (rad)	$V(s)$ (kJ/mol)
1.249	1.915	–2.936	–1.827	8.5
1.090	1.090	–2.821	1.434	11.8
1.028	–1.045	1.270	–0.094	13.5
1.247	1.917	–2.946	1.446	14.5
1.090	1.103	–2.847	0.127	15.8
1.246	1.917	–2.947	0.258	18.3

Table S7. CVs of inner structures and bias potentials of the EQ points of the NATA in $z = 30$ Å.

ϕ (rad)	ψ (rad)	χ_1 (rad)	χ_2 (rad)	$V(s)$ (kJ/mol)
–1.396	–1.009	–3.033	–1.970	–64.7
–1.434	2.074	–3.038	–1.970	–63.2
–1.397	–1.009	–3.041	1.488	–61.0
–1.391	–0.999	–1.026	1.924	–60.6
–1.435	2.075	–3.047	1.488	–59.5
–1.426	2.078	–1.027	1.925	–59.4
–1.391	–0.998	–1.023	–1.599	–59.1
–1.508	1.149	–1.025	1.924	–58.1
–1.426	2.078	–1.025	–1.599	–57.8
–1.431	2.770	–1.016	1.922	–56.8
–1.508	1.148	–1.023	–1.599	–56.5
–1.431	2.771	–1.013	–1.601	–55.2
–1.239	–0.425	1.052	1.687	–52.3
–1.295	2.869	1.017	1.687	–51.9
–1.234	–0.433	1.068	–1.579	–49.9
–1.291	2.867	1.029	–1.585	–49.4
–2.556	2.942	0.958	1.689	–48.6
–1.486	1.045	0.913	1.692	–47.9
–2.556	2.942	0.962	–1.596	–46.0
1.206	–1.147	–2.976	–1.969	–45.6
–2.447	0.988	0.900	1.693	–45.6
–1.488	1.046	0.908	–1.605	–45.3
0.997	0.963	–0.947	1.910	–44.0
1.197	–1.186	–0.965	1.913	–43.2
–2.447	0.990	0.894	–1.607	–43.0
0.997	0.961	–0.940	–1.617	–42.5
1.205	–1.147	–2.984	1.485	–41.8
1.197	–1.186	–0.958	–1.613	–41.6
1.000	1.096	–2.923	–1.967	–41.6
–1.226	–0.448	1.093	0.009	–41.2
–1.283	2.862	1.054	0.068	–40.6
1.058	–1.971	–0.969	1.914	–39.5

Table S7. CVs of inner structures and bias potentials of the EQ points of the NATA in $z = 30$ Å.

Continued.

ϕ (rad)	ψ (rad)	χ_1 (rad)	χ_2 (rad)	$V(s)$ (kJ/mol)
1.057	–1.977	–0.963	–1.611	–38.0
1.000	1.098	–2.927	1.485	–37.8
–2.556	2.940	0.985	0.172	–37.1
–1.477	1.038	0.932	0.257	–36.3
1.192	2.974	–0.946	1.910	–35.1
–2.447	0.983	0.912	0.292	–33.9
1.192	2.975	–0.938	–1.617	–33.6
0.649	0.954	1.000	1.688	–32.9
–1.223	–0.454	1.102	–3.108	–31.3
–1.288	2.865	1.037	–3.032	–30.8
0.650	0.952	1.009	–1.589	–30.4
–1.652	–2.031	0.921	0.276	–27.9
0.656	–2.056	1.000	1.688	–27.0
0.658	–2.062	1.009	–1.588	–24.4
0.982	3.075	1.126	1.689	–22.9
1.027	–1.024	1.182	–1.563	–21.6
0.654	0.945	1.031	0.103	–21.5
0.990	3.071	1.150	–1.567	–20.6
0.662	–2.077	1.032	0.103	–15.6
1.062	–0.878	1.269	–0.316	–13.4
1.001	3.066	1.186	–0.144	–12.2
0.649	0.954	1.000	–2.985	–11.7
0.656	–2.056	1.001	–2.986	–5.8

References

(1) Mitsuta, Y.; Shigeta, Y. Analytical Method Using a Scaled Hypersphere Search for High–Dimensional Metadynamics Simulations. *J. Chem. Theory Comput.* **2020**, *16* (6), 3869–3878. https://doi.org/10.1021/acs.jctc.0c00010.

(2) Biarnés, X.; Pietrucci, F.; Marinelli, F.; Laio, A. METAGUI. A VMD Interface for Analyzing Metadynamics and Molecular Dynamics Simulations. *Comput. Phys. Commun.* **2012**, *183* (1), 203–211. https://doi.org/10.1016/j.cpc.2011.08.020.

(3) Noé, F.; Horenko, I.; Schütte, C.; Smith, J. C. Hierarchical Analysis of Conformational Dynamics in Biomolecules: Transition Networks of Metastable States. *J. Chem. Phys.* **2007**, *126* (15). https://doi.org/10.1063/1.2714539.